scientific reports

Check for updates

OPEN

Long-term benefits of TUDCA supplement in ARSACS zebrafish model

Valentina Naef[1]✉, Stefania Della Vecchia[1], Michela Giacich[1], Rosario Licitra[2], Tiziana Bachetti[3], Gabriela Coronel Vargas[3], Marco Ponassi[3] & Filippo Maria Santorelli[1]✉

Autosomal recessive spastic ataxia of Charlevoix-Saguenay (ARSACS) is an early-onset neurodevelopmental and neurodegenerative disorder characterized by ataxia, spasticity, and peripheral neuropathy. However, several studies have highlighted that some patients also experience cognitive, emotional and social deficits, suggesting a more complex clinical picture that extends beyond motor symptoms. Building on these findings, this study aimed to: (i) investigate locomotor, social and cognitive deficits in adult *sacs*$^{-/-}$ zebrafish versus wild-type (WT) controls through behavioural tests; (ii) identify molecular patterns associated with the adult disease phenotype using transcriptomic and proteomic analyses of *sacs*$^{-/-}$ and WT brains; (iii) evaluate the effectiveness of long-term treatment with tauroursodeoxycholic acid (TUDCA) on behavioural outcomes and omics profiles in the zebrafish *sacs*$^{-/-}$ model. Our findings indicate impairments in cognitive, social, and emotional behaviors in aged *sacs*$^{-/-}$ zebrafish, which resemble some deficits observed in human patients. Transcriptomic and proteomic analyses of adult brains identified alterations in genes related to circadian rhythms and neuroinflammation. Notably, disruptions in sleep and circadian rhythms are frequently reported in individuals with cerebellar ataxia and may contribute to cognitive and behavioral changes. Long-term treatment with TUDCA, a neuroprotective molecule, was associated with partial improvements in social and cognitive behaviors and modifications in omics profiles in the zebrafish model. These results support the potential of further exploring TUDCA in future preclinical and clinical studies, while also emphasizing the need for additional investigations to better understand its mechanisms of action.

Keywords ARSACS, Ataxia, Zebrafish, Neurodegeneration, TUDCA

Autosomal recessive spastic ataxia of Charlevoix–Saguenay (ARSACS) is a distinct form of hereditary early-onset spastic ataxia characterized by progressive degeneration of the cerebellum and spinal cord due to mutations in the *SACS* gene[1]. The *SACS* gene encodes sacsin, a large multidomain protein with a molecular weight of 520 kDa[2]. Sacsin is among the largest proteins encoded by the human genome, though its complex multidomain structure has only been partially characterized[3,4]. It is believed that sacsin plays a role in protein quality control, which may influence both neurodevelopment and neurodegeneration. However, despite the identification of several structural domains, the precise function of sacsin and the pathophysiological consequences of its dysfunction remain largely uncharacterized. Alongside the motor symptoms, which typically include the triad of ataxia, spasticity and peripheral neuropathy, some individuals with ARSACS exhibit intellectual disabilities and behavioural abnormalities[5]. Cerebellar defects resemble the features of cerebellar cognitive-affective syndrome (CCAS), a condition characterized by deficits in executive functioning, spatial cognition, language abilities and emotional regulation[1,6,7]. Mouse models of ARSACS have been developed, exhibiting progressive deficits in motor coordination that closely mirror the ataxia-like symptoms of the disease[8]. However, data on cognitive and behavioural aspects remain scarce. Recently, Chen and colleagues generated double knockout mice for *Sacs*/Bβ2 and *Sacs*/Akap1, to test behavioural modifications related to ARSACS, and observed a significant decline in cognitive abilities in older *Sacs* knock-out mice[9]. Their study provided the first experimental evidence linking ablation of the *SACS* gene not only to motor impairments but also to learning and memory deficits, laying the foundations for further investigation of this area[9]. Zebrafish possess a range of neurobehavioral traits that are translationally relevant. Zebrafish, are also increasingly recognized as suitable organisms for modelling

[1]Neurobiology and Molecular Medicine, IRCCS Fondazione Stella Maris, 56128 Pisa, Italy. [2]Department of Veterinary Sciences, University of Pisa, 56124 Pisa, Italy. [3]IRCCS Ospedale Policlinico San Martino, 16132 Genoa, Italy. ✉email: valentina.naef@gmail.com; filippo3364@gmail.com

neurodegenerative diseases, and thus as a valuable platform for exploring disease mechanisms and testing potential treatments[10]. Despite comprehensive definition of non-motor symptoms in patients with ARSACS, in model mice, and in the zebrafish^{R487Kfs*495} KO strain[11]the pathophysiology and underlying mechanisms of the disease remain poorly understood. Although the cerebellum plays a role in the retrieval of episodic memory and in other cognitive tasks[12]it is still unclear how it contributes to cognitive and affective deficits. Currently, there are no definitive treatments available for degenerative ataxia[13]and options for addressing the progressive degeneration of Purkinje cells in patients are limited. The repurposing of FDA-approved drugs with the potential to act on multiple molecular targets is a promising avenue to explore at preclinical level. Aged mice treated with tauroursodeoxycholic acid (TUDCA) (300 mg/kg) exhibited enhanced energy expenditure, improved metabolic flexibility and better cognitive abilities[10]. Additionally, in a chronic Parkinson's disease model exhibiting significant dopaminergic degeneration, pretreatment with TUDCA(500 mg/kg, intraperitoneally) protected against neuronal damage and mitigated the activation of microglia and astroglia[14]. On the basis of this previous evidence, we investigated whether dietary supplementation with TUDCA could improve the phenotype of our published zebrafish model of ARSACS[11,15]. We showed that TUDCA significantly improved motor coordination, social interaction and cognitive impairments in this model. We found that TUDCA influences omics profiles in our zebrafish model. Transcriptomic and proteomic analyses suggest that TUDCA may modulate key cellular processes, including stress response, protein quality control, membrane stability, inflammation, and cytoskeletal dynamics. TUDCA could have potential benefits in improving locomotor and cognitive functions while also affecting molecular pathways related to neuroinflammation and cellular homeostasis. However, further studies will be necessary to validate these findings and better characterize the metabolic and functional effects of TUDCA. Overall, this study supports the need for further investigation into TUDCA's potential therapeutic effects.

Results

TUDCA improves early survival in *sacs*$^{-/-}$ zebrafish without affecting growth or morphology

ARSACS is an incurable condition that requires ongoing research to identify potential treatments and interventions. As a proof of concept, we tested a diet supplemented with TUDCA in *sacs*$^{-/-}$ zebrafish (Fig. 1A). This experimental diet was based on this compound's previously documented neuroprotective and anti-inflammatory properties[16]. During the first month of life—a critical period typically characterized by high mortality in our ARSACS model—we observed a significant improvement in survival rates. Notably, after this critical window, survival stabilized over time (Fig. 1B). To exclude potential metabolic side effects, particularly since TUDCA had not previously been tested in zebrafish over such a long period before, we assessed the fish at three months of age. No significant morphological abnormalities or changes in body weight were observed when comparing the *sacs*$^{-/-}$ mutants to the TUDCA-treated *sacs*$^{-/-}$ group. TUDCA treatment seemed to ameliorate the growth of the untreated mutants. (Fig. 1C).

TUDCA treatment enhances locomotor activity and reduces anxiety in *sacs*$^{-/-}$ zebrafish

At the larval stages, we found that the *sacs*$^{-/-}$ zebrafish exhibited symptoms resembling motor impairments observed in humans with ARSACS[15]. Using the novel tank diving test (Fig. 2A), we observed that one-year-old *sacs*$^{-/-}$ zebrafish, similar to *Sacs*$^{-/-}$ mice[17], displayed reduced speed of movement and impaired motor control (Fig. 2B). Active behaviour driven by the innate motivation to explore unfamiliar surroundings constitutes a typical normal response to a novel environment[18]and is a trait evolutionarily conserved across many species[19]. However, adult *sacs*$^{-/-}$ zebrafish exhibited anxiety, a passive response characterized by a prolonged time spent in the lower half of the tank, and thus reduced exploratory activity (Fig. 2C), which suggested a decline in their ability or motivation to explore new environments. To further assess anxiety-related behavior, we employed the open-field test (Fig. 2D), which provides complementary information to the novel tank diving test by specifically evaluating thigmotaxis (or "wall-hugging")[19]. In this test, we analysed the exploratory behaviour of adult *sacs*$^{-/-}$ zebrafish observing that TUDCA-treated *sacs*$^{-/-}$ zebrafish showed a moderately enhanced exploratory and locomotor response compared with untreated *sacs*$^{-/-}$ specimens (Fig. 2E). Furthermore, we compared the time spent in the inner zone (centre) versus the outer zone of the tank[19] (Fig. 2F). Wild-type fish habituated more quickly to the environment and exhibited reduced thigmotaxis, indicative of lower anxiety levels. In contrast, adult *sacs*$^{-/-}$ zebrafish were less inclined to venture away from the safety of the edges of the tank and demonstrated heightened anxiety (Fig. 2F). Notably, while TUDCA supplementation seemed to partially rescued the anxiety phenotype, its effects appeared stronger in the novel tank diving test than in the open-field test. This discrepancy may stem from differences in the nature of the two behavioral paradigms. Indeed, the novel tank diving test primarily assesses the acute stress response to a novel environment, with zebrafish typically exhibiting an initial preference for the bottom of the tank before gradually exploring the upper zones. In contrast, the open-field test evaluates thigmotaxis, a behavior driven by long-term anxiety levels and risk assessment, where increased center avoidance indicates heightened anxiety. These findings suggest that TUDCA treatment may potentially lead to partial recovery of both motor and non-motor symptoms in the *sacs*$^{-/-}$ model. It is speculative to hypothesize that the stronger effect observed in the novel tank diving test may indicate that TUDCA primarily improves stress reactivity and exploratory drive rather than directly modulating chronic anxiety-related behaviors.

TUDCA ameliorates social deficits in *sacs*$^{-/-}$ zebrafish

Beyond its role in motor symptoms, recent studies have also highlighted involvement of the cerebellum in cognitive, emotional and social functions[6]. Patients with cerebellar ataxia may exhibit difficulties in social interactions and in understanding others' emotions, which can impact personal relationships and overall quality of life[20]. Direct studies linking cerebellar degeneration to changes in social and cognitive behaviour in ARSACS patients are limited, although impairment of social skills and severe psychiatric symptoms have been reported in

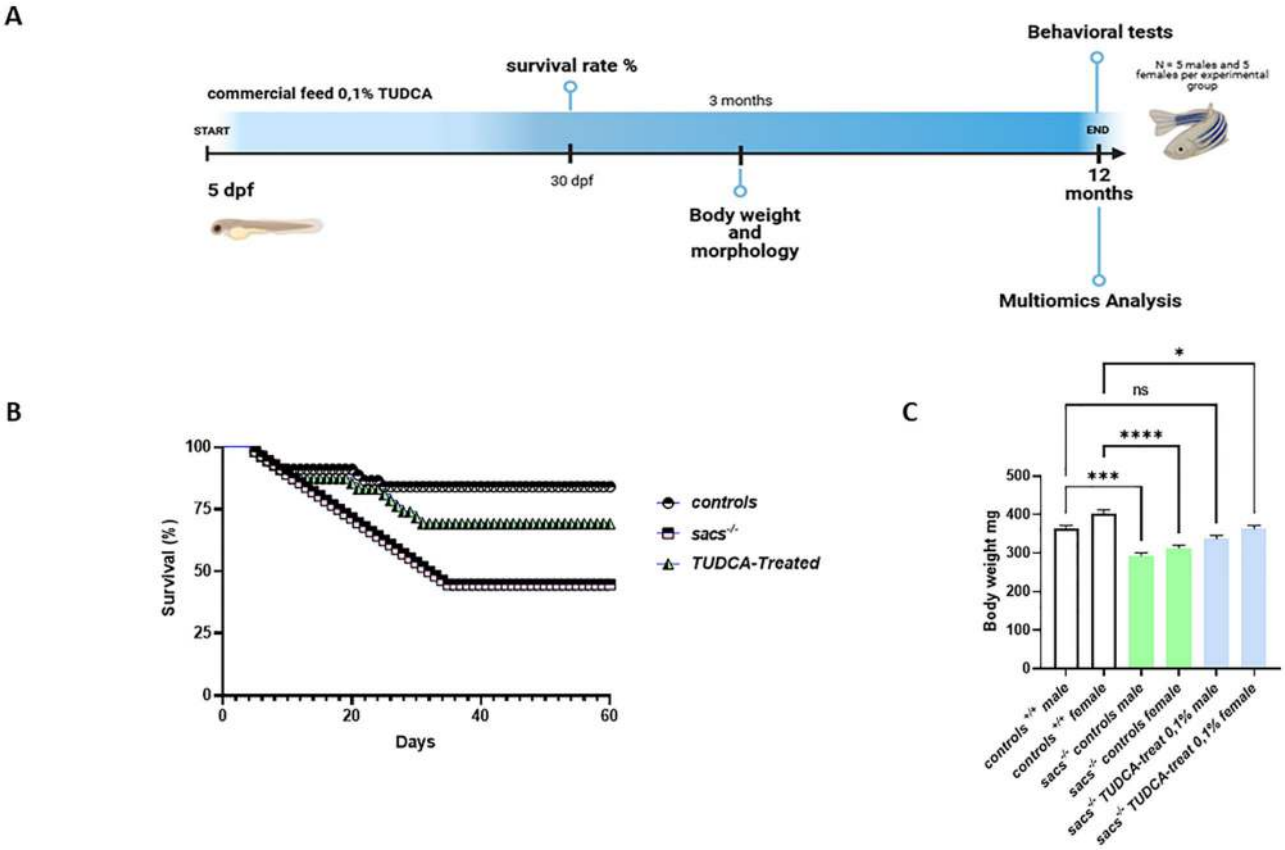

Fig. 1. (**A**) Experimental timeline. Images were created using BioRender, a scientific image and illustration software. Effects of the TUDCA-supplemented diet treatment on the survival rate and growth of juvenile and adult zebrafish modelling ARSACS. (**B**) Kaplan-Meier survival comparison among groups, showing a significant effect of TUDCA in *sacs*$^{-/-}$ treated fish (log-rank (Mantel-Cox) test) ***$p < 0.001$. (**C**) Data are presented as mean ± S.E.M. ($N = 5$ males and 5 females per experimental group). Statistical significance was determined using one-way ANOVA followed by Tukey's multiple comparison test: ns (not significant), *$p < 0.05$, ***$p < 0.001$, **** $p < 0.0001$.

these patients[21,22]. Zebrafish are a highly social species that prefer to spend time in proximity to conspecifics[23]. Their shoaling behaviour serves several adaptive functions, providing protection from predators for example, as well as increasing foraging efficiency and mating success[23]. Interestingly, cerebellar circuits in zebrafish also play an important role in social orienting behaviour[24]. To explore the effect of loss of sacsin on social behaviours, we performed a shoaling test to compare social behaviour between homogeneous groups of zebrafish[25]. In a novel tank, stressed fish tend to swim closer together, maintaining smaller inter-fish distances than non-stressed fish[25]. Indeed, tighter shoals indicate higher anxiety[26]. We measured the average inter-fish distance and found that adult *sacs*$^{-/-}$ zebrafish, compared with WT fish, appeared more stressed, swimming closer together (inter-fish distance of < 6 cm), a trait that reduced their exploratory behaviour (Fig. 3A-B). However, TUDCA-treated *sacs*$^{-/-}$ fish showed greater inter-fish distances than their untreated *sacs*$^{-/-}$ counterparts, demonstrating less anxiety. The social preference and interaction tests were subsequently performed as already described[23] (Fig. 3C-D). During the habituation phase, we continued to observe increased exploratory behaviour in TUDCA-treated versus untreated *sacs*$^{-/-}$ fish. In the test phase, a group of four conspecific zebrafish was placed in the right side of the tank, and a single fish per experimental group was placed in the left side as reported in a previous study[20]. We observed that adult WT zebrafish generally contacted the group on the right side and spent more time in the conspecific sector than the empty sector, showing a strong group-forming tendency[23]. In contrast, *sacs*$^{-/-}$ zebrafish spent their time evenly throughout the tank, exhibiting reduced social contact with the peer group and a lower proportion of time in the conspecific sector (Fig. 3C-D). When treated with TUDCA, however, *sacs*$^{-/-}$ fish showed improved sociability (Fig. 3C-D).

TUDCA improves cognitive performance in the ARSACS zebrafish model

Cognitive symptoms have been reported in some cases of ARSACS[5,27] and in the *Sacs*-KO mouse model[9]. Although fMRI studies indicate that the cerebellum participates in the recovery of episodic memory and other cognitive tasks, and CCAS[12] has been described in ARSACS[6,7,21]it is still not clear how cerebellar disorders impair cognition. Furthermore, most of the genes associated with cerebellar ataxia diseases, including *SACS*, are ubiquitously expressed, and brain atrophy commonly follows cerebellar atrophy in hereditary ataxias[28]. Since

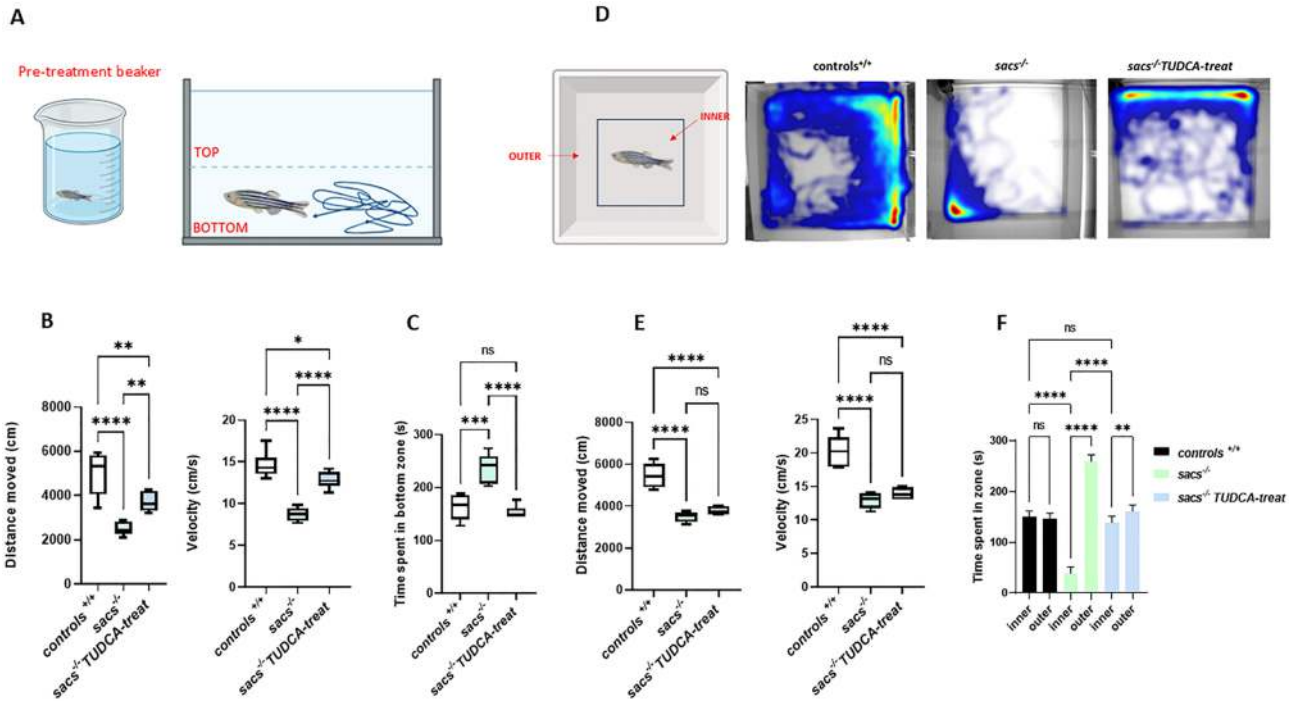

Fig. 2. (**A**) Zebrafish locomotor activity and anxiety-like behaviour during a 5-minute novel tank test. (**B**) Total distance travelled (cm) and average speed while moving (cm/s). (**C**) Time (s) spent in the bottom half of the tank (below dotted line). (**D**) Schematic diagram of the open-field test and thigmotaxis test in adult zebrafish and heat maps. In the analysis of thigmotaxis test, the area of the peripheral zone is equal to the central zone. Single adult fish were placed in an open-field apparatus for 5 min, to quantify their exploration and analyse its pattern. (**E**) Total distance travelled (cm) and average speed while moving (cm/s). Data are presented as box plots, where the central line represents the median, the box indicates the interquartile range (IQR), and the whiskers extend to 1.5 times the IQR. (**F**) Average time spent in zones. Data are presented as mean ± S.E.M. $^{*}p < 0.05$, $^{**}p < 0.01$, $^{***}p < 0.001$, and $^{****}p < 0.0001$ were calculated by ANOVA followed by Tukey's multiple comparison test. ns, no significant difference. Images were created using BioRender, a scientific image and illustration software. ($N = 5$ males and 5 females per experimental group)

zebrafish can be used to model complex human behavioural traits such as reward responsiveness, learning, and memory[29]we took advantage of this characteristic to investigate the potential presence of cognitive impairments in *sacs*$^{-/-}$ mutants. We performed the novel object recognition (NOR) test and analysed the time spent by the animals exploring objects[29] in the open-field test apparatus. The NOR test leverages animals' naturally greater tendency to explore novel objects over familiar ones, and thus explores their curiosity and memory capabilities[30]. Zebrafish possess recognition memory for simple 2- and 3-dimensional geometrical shapes[31]. We placed adult fish in a tank containing two identical blue cubes (Fig. 4A) and allowed them to explore freely for a set amount of time, becoming familiar with the objects present (phase 1, Fig. 4A-B). After training, the animals were submitted to a retention interval of 1 h, then, we put the fish back in same tank, in which we had placed one of the familiar blue objects and a novel object (red cube), and evaluated the amount of time they spent exploring the novel object compared with the familiar one (phase 2, Fig. 4A and B), which is an indicator of their recognition memory[29,30]. In the training session (phase 1), no preference between the two identical blue cubes was observed. In the test session (phase 2) we found that adult WT fish spent more time exploring the novel object, a result indicating memory retention as previously reported[31]whereas adult *sacs*$^{-/-}$ fish did not show a preference between the familiar and novel object (Fig. 4B-C). However, when treated with TUDCA, adult *sacs*$^{-/-}$ zebrafish showed a significant preference for the new object compared with the familiar object ($^{****}p < 0.0001$), which suggests an improvement in their cognitive performance.

Key insights from multiomics analyses in the zebrafish ARSACS model

Understanding early cellular stresses and altered pathways in the brain that may contribute to the onset of ARSACS is crucial for developing preventative treatments. However, obtaining these insights through studies in living humans is challenging. We performed transcriptome analysis comparing whole brains from 12-month-old WT and homozygous *sacs*-mutant fish. 527 genes were differentially expressed in the entire brains of the *sacs*$^{-/-}$ group compared with the WT group (Supplementary File 1). 213 genes showed increased expression and 314 showed decreased expression. Gene ontology (GO) and protein-protein interaction (PPI) analyses revealed enrichment of genes associated with circadian rhythms that have not been reported in other ARSACS models (Fig. 5A-B). Therefore, we performed gene set enrichment analyses (GSEA) to predict which cellular processes were affected. These analyses identified several pathways related to biological processes such as

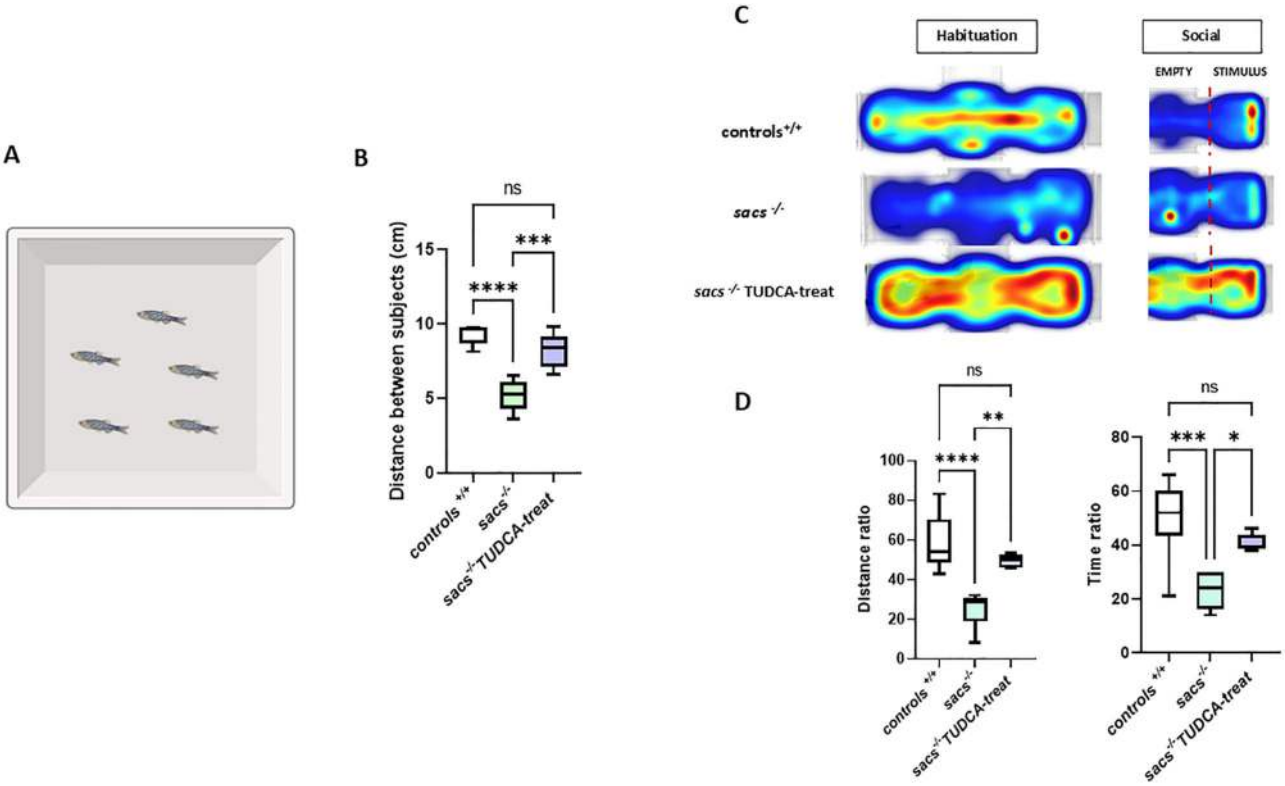

Fig. 3. (**A**) Shoaling test. The test involves placing a group of conspecific fish in a novel tank for 5 min, after an acclimatization time. (**B**) The shoal is video recorded for behavioural analysis, and to quantify social cohesion, which is measured by the average mean distance between members of the group. (**C**) The heat maps show that control zebrafish exhibited a significantly higher frequency of proximity to a group of zebrafish compared with *sacs*$^{-/-}$ zebrafish. Furthermore, pretreatment with TUDCA improved the sociability of *sacs*-deficient fish compared with untreated mutant fish. (**D**) [(Distance Ratio% = distance travelled in the conspecific sector /by the total distance travelled) ×100] and [(Time Ratio %=Time spent in conspecific sector/ total time observed) ×100]. Data are presented as box plots, where the central line represents the median, the box indicates the interquartile range (IQR), and the whiskers extend to 1.5 times the IQR. ($N = 5$ males and 5 females per experimental group). $^{*}p < 0.05$, $^{**}p < 0.01$, $^{***}p < 0.001$ and $^{****}p < 0.0001$ were calculated by ANOVA followed by Tukey's multiple comparison test. ns, no significant difference. Images were created using BioRender, a scientific image and illustration software.

"neuroinflammation" and "response to oxidative stress" (Fig. 6A). PPI analyses revealed downregulation of several proteins related to "mitochondrial activity" and "oxidative phosphorylation" (Fig. 6B), consistent with mitochondrial dysfunction as reported in the literature[32–34]. The overlap between our results and those reported in the literature further supports the potential of our model in modelling ARSACS pathology.

To gain a more comprehensive understanding of the molecular alterations in our model and evaluate potential downstream effects at the protein level, we performed proteomic analysis on adult brains. This analysis revealed a complex network of upregulated and downregulated proteins, which could indicate potential neurodegenerative molecular changes in *sacs*$^{-/-}$ adult zebrafish, which could be further explored in future studies. In (Tables 1 and 2), we highlighted significant proteins associated with biological processes that are altered in ARSACS pathology in others model, as previously described in[35]. In particular, we found an imbalance in key processes such as "Mitochondrial Function", "Oxidative Stress", "Neuroinflammation", "ER Stress" and "Synaptic Signalling" that, in combination with alterations in circadian patterns, could exacerbate neuronal damage, leading to a cycle of chronic stress and inflammation in the brain[36]. Notably, these same pathways have also emerged in previous in vitro studies in ARSACS primary cells, further supporting their relevance to disease pathophysiology[37] .

TUDCA modulates gene expression and protein regulation in the ARSACS zebrafish model

To gain a better understanding of diet-induced changes in whole-brain gene expression, we performed RNA-seq analysis. A comparative analysis between *sacs*$^{-/-}$ and TUDCA-treated *sacs*$^{-/-}$ zebrafish indicated that dietary supplementation with TUDCA may be associated with modifications in gene expression signatures related to circadian rhythm and neuroinflammatory pathways. As reported in the literature, we found that TUDCA may play a multifaceted role in supporting metabolic health. In particular, as previously reported, it appears to influence cholesterol and fat metabolism, reducing the *ER Stress*[64] that occurs when misfolded proteins accumulate. Of 817 genes differentially expressed in the whole brains of the TUDCA-treated *sacs*$^{-/-}$ group compared with the untreated *sacs*$^{-/-}$ fish, 422 showed increased expression, while 395 exhibited decreased expression

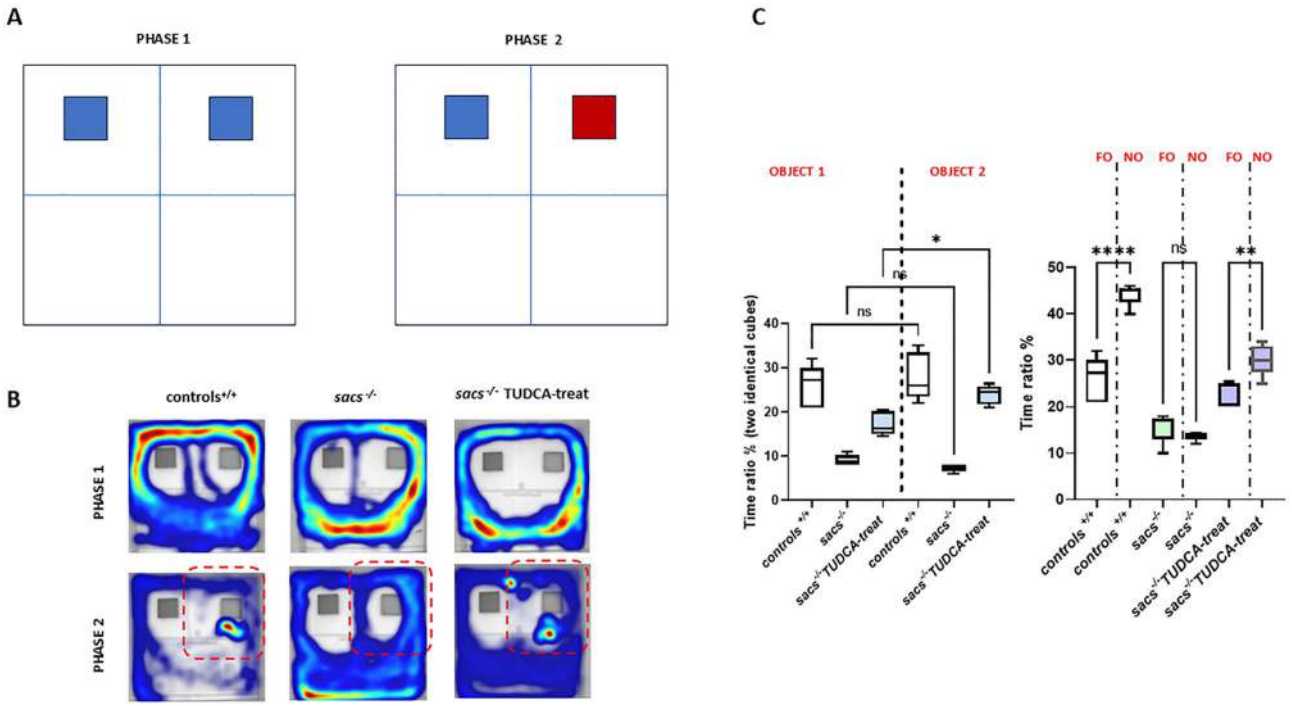

Fig. 4. (**A**) Schematic diagram of the novel object recognition test. (**B**) The heat map shows that adult *sacs*$^{-/-}$ zebrafish fed with TUDCA exhibited a significant preference for exploration of the novel object, similar to adult controls. Instead, untreated adult *sacs*$^{-/-}$ zebrafish did not show a preference between the familiar and novel object. (**C**) The exploration time of each object (%) was analyzed during training between two identical objects 1 and 2 and between the new object (**NO**) and the familiar object (**FO**) in the test session. Data are presented as box plots, where the central line represents the median, the box indicates the interquartile range (IQR), and the whiskers extend to 1.5 times the IQR. ($N = 5$ males and 5 females per experimental group). ns, no significant difference, *$p < 0.05$, **$p < 0.01$, ***$p < 0.001$ and ****$p < 0.0001$ were calculated by ANOVA followed by Tukey's multiple comparison test.

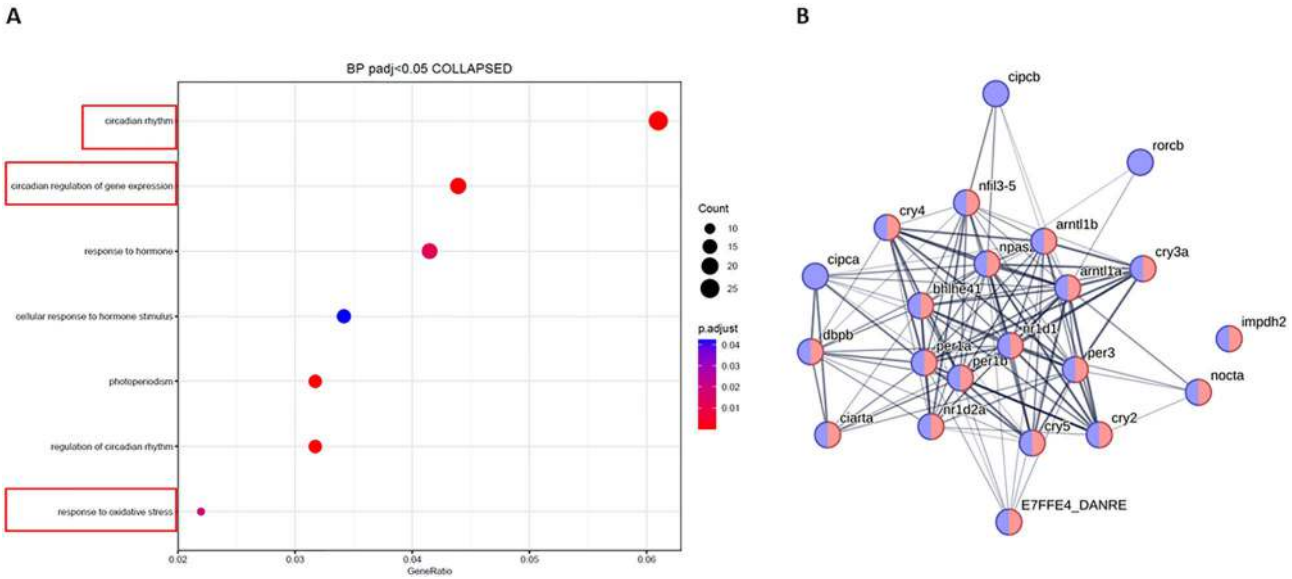

Fig. 5. (**A**) The top 20 enriched GO biological process categories were plotted. (**B**) Protein-protein interaction analysis using the STRING bioinformatic suite (https://string-db.org/) revealed an enrichment of genes associated with circadian rhythms. Network nodes represent proteins involved in rhythmic processes (blue) and circadian rhythms (red). The edges represent protein-protein associations, with thickness indicating the strength of data support. PPI enrichment *p*-value:< 1.0e-16.

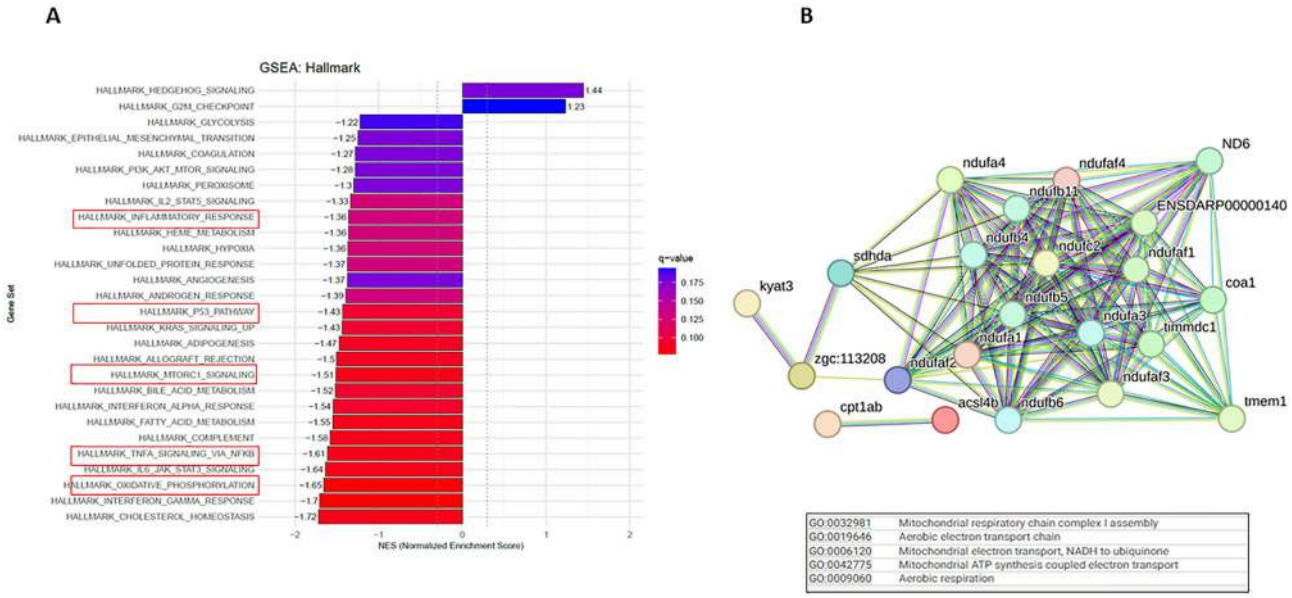

Fig. 6. (**A**). GSEA in adult *sacs*$^{-/-}$ zebrafish brains compared with WT. (**B**) Protein-protein interaction analysis using the STRING bioinformatic suite (https://string-db.org/) revealed an enrichment of down-regulated genes associated with mitochondrial function. Network nodes represent proteins and each node represents all the proteins produced by a single, protein-coding gene locus. The edges represent protein-protein associations, with thickness and colors indicating the strength of data support. PPI enrichment *p*-value:< 1.0e-16.

Gene	Category	Function	Refs.
MT2	Oxidative Stress	Anti-inflammatory, and anti-apoptotic agent	38,39
FLAD1	Oxidative Stress	Cofactor in redox reactions	40,41
UOX	Oxidative Stress	Involved in the urate catabolic process, an antioxidant pathway reducing oxidative damage	42
MRPS15	Oxidative Stress	Involved in pathways related to mitochondrial translation and protein metabolism	43,44
VPS18	ER Stress	Involved in protein trafficking and lysosomal degradation	45
CYP22K6	Oxidative Stress	Involved in oxidative metabolism	46
TSR2	ER Stress	Involved in apoptosis	47
TRNT1	ER Stress	Linked to ER stress and increased oxidative stress	48,49
TBCE	ER Stress	Involved in microtubule cytoskeleton organization	50
CRP	Neuroinflammation	Marker of neuroinflammation and peripheral inflammation	51
FABP10A	Neuroinflammation	Involved in fatty acid transport	52,53

Table 1. List of upregulated proteins identified through proteomics analysis in the brains of adult *sacs*$^{-/-}$ zebrafish compared with wild-type (WT) counterparts.

Gene	Category	Function	Refs.
MT-ND2	Mitochondrial Function	Core subunit of the mitochondrial membrane respiratory chain NADH dehydrogenase (Complex I)	54
MT-CO1	Mitochondrial Function	Part of respiratory chain complex IV, involved in ATP synthesis coupled electron transport	55
MCTS1	Cell Cycle Regulation and Apoptosis	Involved in the regulation of various processes, including cell cycle modulation and apoptosis	56
B2M	Immune Regulation	Subunit of major histocompatibility complex (MHC) class I	57,58
OPTN	Neuroinflammation & Cell Death	Involved in various vesicular trafficking pathways	59
HPX	Oxidative Stress	Involved in protecting cells from oxidative stress	60
TRAPPC2	Intracellular Vesicle Trafficking	Involved in the targeting and fusion of endoplasmic reticulum-to-Golgi transport vesicles	61,62
DYNC1I2A	Retrograde Transport	Acts as a retrograde microtubule motor to transport organelles and vesicles	63

Table 2. List of downregulated proteins identified through proteomic analysis in the brains of adult *sacs*$^{-/-}$ zebrafish compared with wild-type (WT) counterparts.

(**Supplementary file 2**). GO analysis revealed differentially expressed genes mainly related to "Developmental Growth", "Lipid Metabolism" and "Intermediate Filament Cytoskeleton Organization" (Fig. 7A). GSEA revealed an enrichment of genes related to categories such as "Lipid Metabolism" and "Oxidative Phosphorylation" (Fig. 7B).

PPI analysis revealed 150 upregulated genes that are functionally related to "Lipid Metabolism" (highlighted in red, Fig. 8A), "Oxidative Phosphorylation" (highlighted in green, Fig. 8A) or "Neurotransmitter and Synaptic Transmission" (highlighted in blue, Fig. 8A). "Oxidative activity/removal of superoxide radical" (highlighted in green, Fig. 8B), "cell redox homeostasis" (highlighted in pink/yellow, Fig. 8B), "mitochondrion organization" (highlighted in red, Fig. 8B), which may indicate a protective and adaptive effect aimed at maintaining redox homeostasis and preventing cellular damage after TUDCA treatment. These results could support the ability of TUDCA to mitigate oxidative stress in our ARSACS model, as previously described[16] .

We performed transcriptome analysis f TUDCA-treated *sacs*$^{-/-}$ zebrafish with that of WT fish (Supplementary File 3). This analysis indicated that the transcriptomic profile of treated mutants did not fully overlap with that of WT fish, suggesting that while TUDCA may ameliorate some molecular alterations, it does not completely restore the WT-like state. Specifically, GSEA analysis identified enrichment in pathways related to biological processes such as "developmental growth", "connective tissue development", "tissue regeneration", and "cytoskeletal organization" (Supplementary Fig. 1A). PPI analysis further revealed an upregulation of genes associated with "cell cycle regulation", "cytoskeletal organization" (highlighted in Yellow), "chromatin remodelling" (highlighted in red), and "neurodevelopmental processes" (highlighted in green). These changes could reflect a compensatory response aimed at mitigating aspects of neurodegeneration (Supplementary Fig. 1B). Additionally, we observed higher expression of genes related to "mitophagy" (highlighted in violet), which aligns with the proposed role of TUDCA in promoting mitochondrial quality control (Supplementary Fig. 1B). Interestingly, we also identified alterations in "RNA processing" and "splicing pathways" among the downregulated genes, suggesting that key gene regulatory mechanisms remain impaired despite TUDCA treatment (Supplementary Fig. 2A). In contrast, immune-related pathways, including "cytokine production" and "immune response signaling", were downregulated, indicating a potential anti-inflammatory effect of TUDCA (Supplementary Fig. 2B). These findings suggest that, while TUDCA partially mitigates specific molecular deficits, it does not fully normalize the transcriptional landscape, highlighting both its therapeutic potential and its limitations in reversing ARSACS-associated dysregulation.

To evaluate downstream effects at the protein level we analysed proteomic data. We identified differentially expressed proteins related to several processes such as "Autophagy" and "Lysosomal Function", "Protein Degradation", "Oxidative Stress Response", "Lipid Transport" and "Metabolism". The upregulation of proteins related to processes like "Synaptic Integrity" and "Synaptic Plasticity", such as SCRIB and CNTN5, is intriguing (Table 3).

Discussion

Beyond the motor dysfunction caused by the progressive cerebellar degeneration, some patients with ARSACS disease exhibit cognitive impairment and behavioural problems[5] including apathy, dysphoria, paranoid thoughts, irritability, and significant cognitive impairment[86]. Several research has demonstrated that cerebellar damage often leads to cognitive deficits and to affective problems, thereby highlighting the cerebellum's significant role in cognitive and emotional processes[87]so that the concept of CCAS-like has been proposed to describe cognitive and emotional alterations linked to cerebellar dysfunction in some instances[6,88]. Although the cognitive and

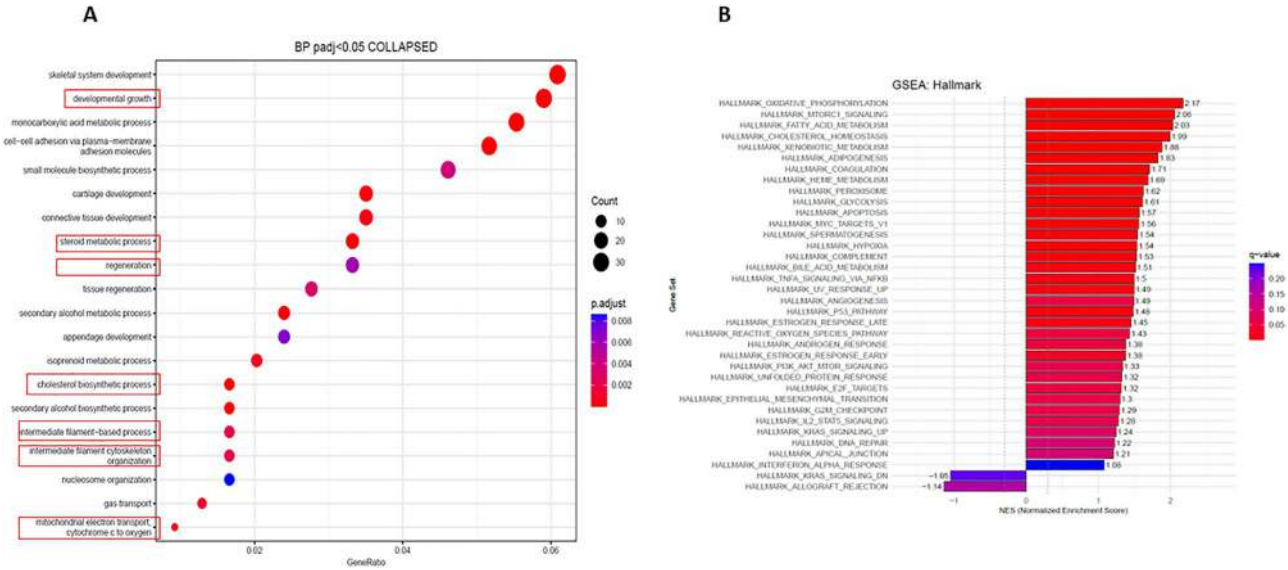

Fig. 7. (**A**) The top 20 enriched GO biological process categories were plotted. (**B**). GSEA in the brains of TUDCA-treated *sacs* vs. WT adult *sacs*$^{-/-}$ zebrafish.

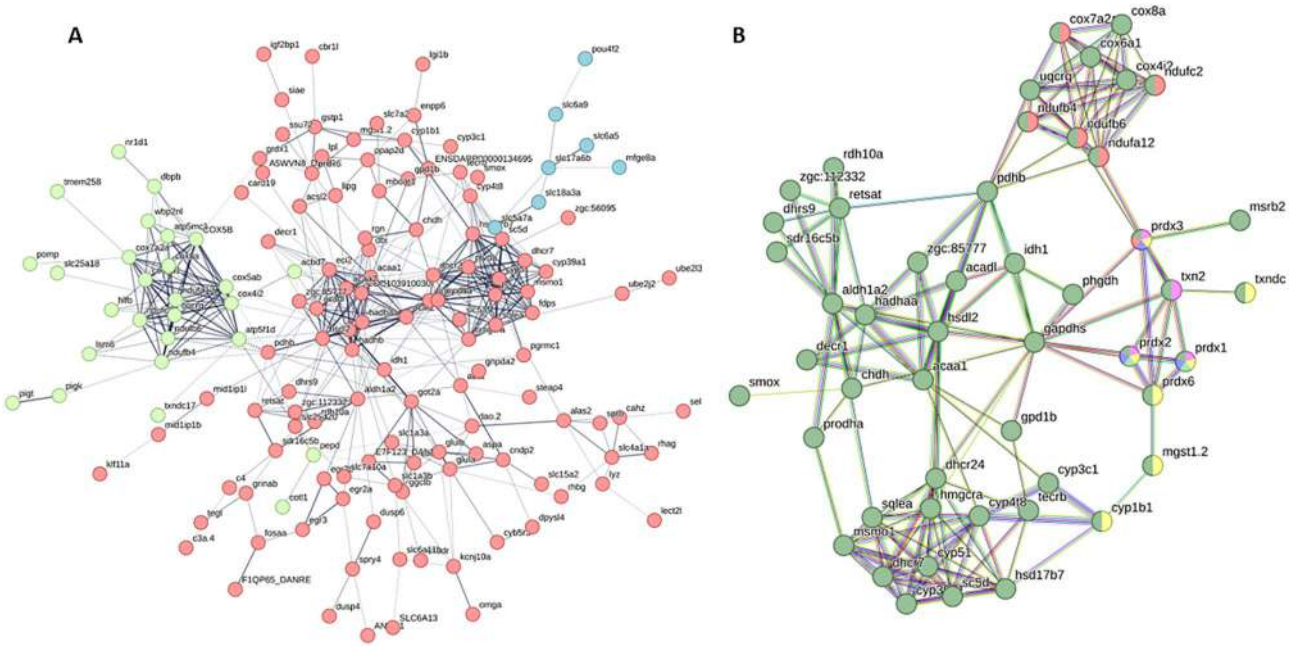

Fig. 8. Protein-protein interaction analysis using the STRING bioinformatic suite (https://string-db.org/) in the brains of treated vs. untreated adult *sacs*$^{-/-}$ zebrafish. (**A**) "Lipid Metabolism" (highlighted in red), "Oxidative Phosphorylation" (highlighted in green) and "Neurotransmitter and Synaptic Transmission" (highlighted in blue). (**B**) "Oxidative activity/removal of superoxide radical" (highlighted in green), "cell redox homeostasis" (highlighted in pink/yellow), "mitochondrion organization" (highlighted in red). Network nodes represent proteins and each node represents all the proteins produced by a single, protein-coding gene locus. The edges represent protein-protein associations, with thickness indicating the strength of data support. PPI enrichment *p*-value:< 1.0e-16.

Gene	Category	Function	Refs.
LAMP5	Protein Trafficking	Involved in establishment of protein localization to organelle	65
USP46	Protein Degradation	Involved in protein deubiquitination and regulation of GABAergic synaptic transmission	66
SCRIB	Synaptic Stability	Involved in neuronal stability and synaptic integrity, maintaining neural connections even under neurodegenerative stress	67,68
CNTN5	Synaptic Plasticity	Involved in the formation of axon connections in the developing nervous system	69,70
HYCC1	Myelination	Involved in neuron-to-glia signalling to initiate or maintain myelination	71
CLPTM1L	Lipid Metabolism	A scramblase that moves GlcN-PI across the ER membrane, aiding glycosylphosphatidylinositol (GPI) biosynthesis, which is essential for protein post-translational modification	72
TMEM11	Mitochondrial Function	Localizes to the outer mitochondrial membrane where it regulates BNIP3/BNIP3L-dependent receptor-mediated mitophagy	73
NXN	Antioxidant Defence	Member of the thioredoxin superfamily, a group of small, multifunctional redox-active proteins	74
PTDSS1	Cell Signalling	A phospholipid found in membranes that plays a role in various cellular functions, including development, cell communication, programmed cell death	75

Table 3. List of upregulated proteins identified through proteomic analysis in the brains of TUDCA-treated vs. untreated *sacs*$^{-/-}$ zebrafish. These changes suggest a putative improvement in brain function in our ARSACS model, leading to an enhancement of behaviours related to learning, memory and social interaction. Downregulation of immune-related proteins like B2M and IFI30 suggest a possible dampening of inflammatory responses, in accordance with tudca's known anti-inflammatory properties[16]. Additionally, the level of reduction of proteins related to the ubiquitin-proteasome system, such as MARCHF2, demonstrates the potential of TUDCA to reduce proteotoxic stress, likely by stabilizing protein folding and minimizing protein accumulation[76,77] (Table 4). These results suggest that TUDCA could exert neuroprotective effects through multiple cellular pathways, potentially slowing down disease progression and improving motor and cognitive function in our model. However, to confirm these speculative findings, further studies will be necessary to validate the obtained results.

Gene	Category	Function	Refs.
B2M	Immune Regulation	An important subunit of major histocompatibility complex (MHC) class I Downregulation may impair immune response.	78
AGR2	Protein Folding	A member of the disulfide isomerase (PDI) family of proteins found in the endoplasmic reticulum	79
MTTP	Lipid Metabolism	This protein is crucial for lipoprotein formation. Putative inhibitor of ferroptosis	80
VPS25	Protein Sorting	Component of ESCRT-I. Selectively modulates FGF signalling by directing receptor sorting through endosomes	81
MARCHF2	Ubiquitination	Member of the MARCH family of membrane-bound E3 ubiquitin ligases	82,83
ARPIN	Cytoskeleton and Cell Motility	Involved in directional locomotion, it regulates actin filament dynamics.	84
FABP10A	Lipid Transporter	Involved in intracellular binding and trafficking of long fatty acids in the liver	52,53
IFI30	Inflammation	Involved in antigen processing	85

Table 4. List of downregulated proteins identified through proteomic analysis in the brains of TUDCA-treated vs. untreated adult *sacs*$^{-/-}$ zebrafish.

affective phenotype observed in ARSACS patients is complex and goes beyond the definition of CCAS, cerebellar dysfunction may contribute to its development[21,22]. In line with findings in *Sacs*-KO mice[9]we observed that loss of sacsin in zebrafish not only affects locomotor activity but also leads to anxiety-like behaviour, social impairment and deficits in object recognition memory. Our findings further strengthen the evidence that loss of sacsin is linked to significant cognitive deficits that become apparent in adulthood. These results reflect the multifaceted role of sacsin in maintaining neural function and suggest that its absence may disrupt critical pathways involved in cognitive processing. The cognitive impairments observed fit into the broader spectrum of neurological abnormalities associated with sacsin deficiency, highlighting the need for continued research to unravel the underlying mechanisms. Our second focus, through transcriptomic and proteomic analyses, was to identify molecular pathways that may be altered in adult *sacs*$^{-/-}$ fish compared with their WT counterparts. This approach aimed to provide deeper insights into the neurobiology of neurodegeneration in our ARSACS model. Dysregulation of the mitochondrial fission enzyme is recognized as a primary driver of the disease; however, since this is a neurodegenerative disorder, other molecular pathways and mechanisms likely contribute simultaneously, worsening both motor and behavioural symptoms and further aggravating the overall progression. In this study, we provide novel insights into the molecular mechanisms underlying ARSACS and their contribution to disease progression. Through RNA transcriptomic analysis of 1-year-old *sacs*$^{-/-}$ zebrafish brains, we identified significant alterations in the expression of circadian rhythm-related factors, such as PER and CRY family genes, as well as other genes related to neuroinflammation. Circadian rhythms direct a wide range of physiological functions, and alterations of them directly affect human health[89]. On the other hand, neuroinflammation could be a key player in the progression of ARSACS. Notably, several studies have found that alteration of the circadian cycle is closely related to the body's inflammatory response, and in the context of neurodegenerative disorders creates a feedback loop that may exacerbate neurodegenerative progression[90]. Immune cells in humans and animals, including microglia, neutrophils, monocytes and lymphocytes, could express clock genes. Thus, circadian cycle alterations may be an important factor mediating central and peripheral inflammatory responses[90]. Disruption of circadian rhythms and neuroinflammation might contribute to neurodegeneration and to clinical manifestations like cognitive impairment[91,92] as observed in our *sacs*$^{-/-}$ zebrafish model. Proteomic analyses highlighted the interplay occurring between upregulated and downregulated proteins in the brains of 1-year-old *sacs*$^{-/-}$ zebrafish compared with those of WT specimens, which could suggest a dynamic attempt by the neurons to modulate oxidative stress and neurodegeneration, acting on neuroinflammation and synaptic communication. Downregulation of key proteins such as MT-CO1 and HPX worsens the neurons' ability to manage damage. For instance, low levels of HPX, which plays a critical role in iron homeostasis[60]can exacerbate oxidative stress and worsen mitochondrial dysfunction. Furthermore, downregulation of TRAPPC2 may lead to Golgi fragmentation and arrest of anterograde trafficking, thereby impairing Golgi function[62]. The increased presence of pro-inflammatory proteins like CRP and OPTN could suggest a chronic inflammatory state. Although the proteomic analyses did not identify proteins directly involved in the regulation of circadian rhythms such as the core clock players (e.g., CLOCK, BMAL1, PER and CRY), several proteins may indirectly influence circadian rhythms. Circadian rhythms and mitochondrial proteins are known to be closely interconnected[93]influencing protein levels and acetylation of mitochondrial genes, as well as mitochondrial morphology and oxidative phosphorylation[93]. Downregulation of mitochondrial-related genes such as MCTS1, MT-ND2 and MT-CO1 significantly impairs mitochondrial function leading to inefficient mitochondrial respiration, a decline in ATP production, and increased reactive oxygen species (ROS) generation, in turn leading to neurodegeneration[94–96]. Indeed, reduced energy production and accumulation of ROS can further alter circadian rhythms[97]. In this scenario, our study provides preliminary evidence suggesting a potential beneficial effect of long-term treatment with TUDCA, which has previously shown efficacy in other models of neurodegeneration such as Parkinson's disease, Alzheimer's disease and Huntington's disease, acting as a mitochondrial stabilizer, anti-apoptotic agent, and anti-inflammatory compound[98–100]. One of the key mechanisms by which TUDCA works is by reducing ER stress[64]. In a model of chronic unpredictable stress-induced depression, administration of TUDCA was able to improve the anxiety-like and depressive-like behaviour driven by neuroinflammation, oxido-nitrosative stress and ER stress[101]. We administered a TUDCA-enriched diet to *sacs*$^{-/-}$ zebrafish from embryonic development to one year of age. Behavioural tests revealed partial but significant improvements in locomotor activity, social behaviour, and cognitive performance,

highlighting TUDCA's capacity to mitigate both motor and non-motor symptoms of ARSACS. Using a multi-omics approach, TUDCA appears to modulate key molecular pathways involved in the progression of ARSACS, particularly those related to circadian rhythms and neuroinflammation. Transcriptomic and proteomic analyses suggest potential neuroprotective effects of TUDCA, with proteomic data indicating its involvement in stress response, protein quality control, membrane stability, inflammation, and cytoskeletal dynamics. Notably, decreased levels of immune-related proteins like B2M and IFI30 suggest a dampening of inflammatory responses, consistent with TUDCA's known anti-inflammatory properties[102]. In addition, the fatty acid-binding protein FABP10A, which was upregulated in *sacs* adult brains, is downregulated following TUDCA treatment. Given the role of FABPs in lipid metabolism and inflammatory processes[103]this finding suggests that TUDCA may contribute to restoring lipid homeostasis, alleviating metabolic stress in *sacs* mutants. Considering the strong link between lipid dysregulation and neuroinflammation, the reduction in FABP10A expression may indicate a decrease in inflammatory signalling, highlighting a broader impact of TUDCA treatment on neuroinflammatory pathways. Furthermore, the downregulation of ubiquitin-proteasome-related proteins such as SSUH2 and MARCHF2 highlights its potential to alleviate proteotoxic stress by stabilizing protein folding and reducing aberrant protein accumulation. The increased expression of USP46, linked to reduced anxiety and depressive-like behaviours in mouse models[104,105]further suggests that TUDCA may influence proteostasis, and could potentially ameliorate stress responses and cognitive functions. However, when comparing the transcriptomic profile of TUDCA-treated mutants with that of WT fish, we observed that it does not fully overlap with the WT-like transcriptional state. This suggests that while TUDCA ameliorates some molecular deficits, it does not completely restore gene expression patterns to WT levels. This aligns with our behavioral findings, where TUDCA treatment led to partial improvements in locomotor and anxiety-related phenotypes rather than complete normalization. The partial recovery may indicate that TUDCA effectively targets specific pathological mechanisms, such as neuroinflammation and mitochondrial dysfunction, while other molecular disruptions caused by sacsin loss remain unaddressed. Further studies are needed to validate these findings and to better understand the precise mechanisms underlying TUDCA's effects. While the transcriptomic and proteomic analyses conducted in this study provide valuable new insights into the molecular alterations occurring in ARSACS, they do not directly establish causality between the observed changes and disease symptoms and additional functional studies will be required to confirm the specific roles of these altered pathways. In particular, the transcriptomic changes related to circadian rhythms and neuroinflammation should be validated using independent experimental approaches. Moreover, further investigations are necessary to elucidate the cellular and anatomical origins of the non-motor symptoms observed in ARSACS, which remain less well characterized compared to motor deficits. Gaining deeper insight into how these symptoms interact and evolve over time could help identify critical windows for therapeutic intervention and contribute to the development of more targeted treatment strategies.

Methods

Fish husbandry and feeding

The adult *sacs*$^{-/-}$ zebrafish used in this study were generated through CRISPR/Cas9 genome editing in the wild-type AB background. These mutants carry a 10-bp deletion in exon 7 of the *sacs* gene, leading to a frameshift mutation and a premature stop codon at residue 495 (R487Kfs*495). This ensures that both WT and *sacs*$^{-/-}$ zebrafish share the same genetic lineage, minimizing the risk of background-related variability. The wild-type AB strain was obtained from the Department of Veterinary Sciences at the University of Pisa. The homozygous *sacs*$^{-/-}$ zebrafish mutant line was crossed, and the F2 progeny were used to investigate the adult phenotype. The control animals used in the study were from the same batch of offspring as the *sacs*$^{-/-}$ mutants and were genetically similar, except for the loss of function in the *sacs* gene. Animals were kept in automated re-circulating systems (Zebtec, Tecniplast, Italy) with reverse osmosis filtered water equilibrated to reach the species-recommended temperature (28° C ± 2° C), pH (7.0 and 7.5), conductivity and ammonia, nitrite, nitrate and chloride levels. Animals were subjected to a light/dark cycle of 14/10 hours. All experiments were conducted in accordance with the European Union (EU) Directive 2010/63/EU on the protection of animals used for scientific purposes, under the supervision of the Institutional Animal Care and Use Committee (IACUC) of the University of Pisa, and in compliance with the 3R principles. TUDCA (TUDCA, Millipore, Darmstadt, Germany) supplementation was carried out by including the compound in the pelleted feed supplementation was carried out by including the compound in the pelleted feed (inclusion rate 0,1% on a fed basis).The purified drug was added to self-made experimental zebrafish feed according to published indications[106]. In brief, the dry feed was finely ground, mixed with osmosis water containing dissolved trehalose to form a dough, then re-pelleted, dried, and stored in the refrigerator until use[106]. In total, two different diets were prepared: 1 control diet and 1 experimental diet, the latter containing TUDCA acid and sodium salt. The decision to use a 0.1% concentration was based on preliminary dosage/effect experiments on mortality and growth in both WT fish and *sacs* mutant fish, evaluated within the first 60 days of life. The chosen dosage was found to be the most effective. The experimental diet was administered twice daily from 5 dpf until adulthood (12 months). Food was provided every day at the same time, with quantities adjusted according to the fish's age and body weight. Specifically, larvae were fed an amount equivalent to 9–10% of their body weight, juveniles received 6–8%, and adults were fed 5%, following recommendations for dry feed with appropriate protein and energy content, as described in[107]. Control fish were maintained under the same conditions as the treated fish but without exposure to any treatment. To exclude potential metabolic side effects of chronic TUDCA exposure, we performed monthly welfare assessments up to 12 months of age, following the University of Queensland's "*Score Sheet for Scoring Endpoints in Zebrafish*" (https://research-support.uq.edu.au/resources-and-support/ethics-integrity-and-compliance/animal-ethics/monitoring-animals), evaluating several aspects such as free swimming behavior in the tank, body weight, and abdominal swelling. The overall welfare status of the analyzed subjects was determined based on the final score.

At 12 months, the animals used for behavioral and molecular testing at that age did not show any signs of distress or ill health. After completing the behavioral experiments, the fish were sacrificed, and organ dissection was performed on the same day. The extracted brains were preserved under identical conditions and subsequently processed as described in the following section.

RNA-sequencing

For transcriptomic analysis, 4 brains were isolated from adult animals per experimental group. RNA was extracted from individual samples to maintain biological variability according to standard procedures. All animals from each experimental group were sacrificed and harvested on the same day to ensure consistency and avoid batch effects. RNA integrity and concentration were assessed using the RNA 6000 Pico Kit on a Bioanalyzer (Agilent Technologies, Santa Clara, CA). The RNA integrity number was between 5.6 and 8.1 for all samples. Due to partial sample degradation, a ribodepletion approach for RNA-seq analysis was employed. 50ng total-RNA was depleted with *Danio rerio*-specific rRNA probes using the dedicated ribo-Pool panel DP-R024-101 (SiTOOLS Biotech, Planegg, Germany). The depleted RNA was used to prepare the library using the SMARTer Stranded Total RNA-Seq kit v3 (Pico Input-Mammalian, Takara Bio, San Jose, CA). Quality and size of RNA-seq libraries were assessed by capillary electrophoretic analysis with an Agilent 4150 Tape station (Agilent Technologies). Libraries were quantified by real-time PCR against a standard curve with the KAPA Library Quantification Kit (KapaBiosystems, Wilmington, MA). Libraries were pooled at equimolar concentration and sequenced in 150PE on a NovaSeq6000 (Illumina, San Diego, CA), generating an average of 48.3 million fragments per sample. GO and KEGG pathway enrichment analysis of differentially expressed genes with padj < 0.05 were performed using ClusterProfiler (v3.18.1) [101]. Subsequently, the top 20 enriched GO biological process categories were plotted. GSEA were performed to determine the enrichment of specific gene sets retrieved from the Molecular Signatures Database (https://www.gsea-msigdb.org/gsea/msigdb/collections.jsp).

Proteomic analysis

Protein isolation

For proteomic analysis, 4 brains were isolated from adult animals per experimental group. RNA was extracted from individual samples to maintain biological variability according to standard procedures. All animals from each experimental group were sacrificed and harvested on the same day to ensure consistency and avoid batch effects. Zebrafish brains were pottered and passed through a 70-µm diameter filter before undergoing a wash with PBS supplemented with protease inhibitors (20 g/ml leupeptin, 25 g/ml aprotinin, 10 g/ml pepstatin, 0.5 mM benzamide) and phosphatase inhibitor (1 mM Na3VO4, Merck, Darmstadt, Germany, Cat. No. 13721-39-6) followed by centrifugation at 4 °C, 1500 rpm for 15 min. The pellet was then disrupted by RIPA buffer, incubated at 4 °C for 60 min, vortexed four times (once every 15 min), and then sonicated for 30 s. Samples were centrifuged at 13,850 rcf for 10 min and supernatants were collected, measured, and supplemented with the same amount of 20% SDS-6% DTT. Subsequently, they were incubated at 95 °C for 5 min. Once cooled, five volumes of MATF (methanol, acetone, and tributyl phosphate, 1:12:1) were added, and samples were incubated for 1 h with agitation. The total proteins were finally pelleted by centrifugation at 12,000 rcf for 15 min, the supernatants were removed, and the protein precipitates dried for about 30 min at RT. The dried pellets were resuspended in 250 µL of 5% SDS in 50 mM ammonium bicarbonate. After quantification, proteins underwent reduction and alkylation followed by trypsin digestion by using Preomics iST (PreOmics, Billerica, MA).

Mass spectrometry

Tryptic digests were analysed using an Ultimate 3000 chromatography system (Thermo Scientific Instruments, Waltham, MA, USA) equipped with a PepMap RSLC C18 EASY spray column (Thermo Scientific Instruments, Cat. No. 13294749) at a flow rate of 250 nl/min and a temperature of 60 °C. Eluate was analysed by mass spectrometry (MS) using a Q Exactive™ Plus Hybrid Quadrupole-Orbitrap™ mass spectrometer equipped with an Easyspray source (both Thermo Scientific Instruments). The data were acquired, in the mass range of 200–2,000 m/z, in data-dependent (DDA) mode alternating between MS and MS/MS scans, using the software Xcalibur (version 4.1, Thermo Scientific Instruments). To perform MS analysis, the desiccated tryptic digests were resuspended with 1.5 mL of the LC-LOAD component of the iST-BCT kit (PreOmics), and analysed by nano-UHPLC-MS/MS using an Ultimate 3000 chromatography system equipped with a PepMap RSLC C18 EASY spray column (75 mm, 50 cm, 2 mm particle size) (both Thermo Fisher Scientific) at a flow rate of 250 nL/min and a temperature of 60 °C. The mobile phases were: (A) 0.1% v/v formic acid in water, and (B) 80% acetonitrile, 20% water and 0.08% v/v formic acid. A 105-min gradient was selected: 0.0–3.0 min isocratic 2% B; 3.0–7.0 min 7% B; 7.0–65.0 min 30% B; 65.0–78.0 min 45% B; 78.0–83.0 min 80% B; 83.0–85.0 isocratic 80% B; 85.0–85.1 2% B; and finally, 85.1–105.0 isocratic 2% B. After separation, the eluate was sent directly to an Easyspray source connected to a Q Exactive™ Plus Hybrid Quadrupole-Orbitrap™ mass spectrometer (Thermo Fisher Scientific). The data were acquired in DDA mode, alternating between MS and MS/MS scans. The software Xcalibur (version 4.1, Thermo Fisher Scientific) was used for operating the UHPLC/HR-MS. MS scans were acquired at a resolution of 70,000 between 200 and 2000 m/z, with an automatic gain control (AGC) target of 3.0×106 and a maximum injection time (maxIT) of 100 ms. MS/MS spectra were acquired at a resolution of 17,500 with an AGC target of 1.0×105 and a maxIT of 50 ms. A quadrupole isolation window of 2.0 m/z was used, and HCD was performed using 30% normalized collision energy.

Mass spectrometry data analysis

Mass spectrometry data were processed with ProteomeDiscoverer® (v. 2.4.1.15) (Thermo Scientific Instrument, Waltham, MA) using a workflow adapted for LTQ ORBITRAP label-free quantification. Briefly, in the processing step we used the *Danio rerio* - tr_canonical v2022-03-02 database for identifying peptide spectral matches in

MS/MS spectra and concatenated decoy (strict target false discovery rate = 0.01, relaxed target false discovery rate = 0.05 for proteins, peptides and peptide spectral matches). Protein quantification was calculated by summed abundances of peptides, and the differential analysis was performed pairwise ratio-based and t-test background-based using the IMP-apQuant node. After conducting a proteome differential analysis, differentially expressed proteins were identified for each experimental point. These were then used to perform further gene ontology analyses. Data were deposited in the PRIDE repository (PXD058522).

Behavioural analysis

Novel tank

Zebrafish were exposed to the experimental challenge in a pre-treatment beaker before being transferred (via a net) to the novel tank for behavioural observation and phenotyping as previously reported[108,109]. After pre-treatment, zebrafish were placed individually in a 1.5-L trapezoidal tank maximally filled with aquarium water. In these experiments, behavioural activity was recorded for 5 min using a webcam set up in front of the tank to analyse the diving response. The tank was virtually divided into two areas (bottom and top) and time spent in the bottom part was used to assess anxiety-like phenotypes. Zebrafish behavioral activity was recorded (1920 × 1080 px). The videos were analysed using Noldus EthoVision® XT17 tracking software (Noldus Information Technologies, Inc., Leesburg, VA, USA).

Open-field test and thigmotaxis

Behavioural experiments were conducted at between 10 a.m. and 4 p.m. in a 30 × 30 × 30 cm tank with opaque walls and partitions. A video camera was suspended above the tank. Adult zebrafish were allowed to swim for 5 min inside the tank, and 5-min videos were recorded. Thigmotaxis was evaluated as reported elsewhere[110] .

Shoaling test

Behavioural experiments were conducted at between 10 a.m. and 4 p.m. in a 30 × 30 × 30 cm tank with opaque walls and partitions. Adult zebrafish were acclimated to the novel tank apparatus for 5 min before the test, after which 5-min videos were recorded. The shoaling assessment was performed by measuring the inter-fish distance (the average of all distances between each zebrafish in a shoal). The method for measuring inter-fish distance was also based on the analysis provided by Noldus EthoVision® XT17 software. This software tracks the precise position of each fish in the arena over time, allowing for accurate inter-fish distance measurements.

Social preference test

Social preference testing was performed with three chambers as already described[23]. In general, social behaviour is assessed by observing how an individual respond to, or interacts with, a social stimulus. Social preference tests are composed of two operational phases. The first is the habituation phase, during which the tested zebrafish is left alone in a chamber of the test tank to explore the novel environment. The second is the interaction phase, which starts with the introduction of the social stimulus consisting of one, or usually two, small groups of live conspecifics[23]. The zebrafish behaviours were quantified as distance distribution or as presence in a zone adjacent to the group of conspecifics. The time ratio [Time ratio %=Time spent in conspecific sector/ total time observed)×100]. The distance ratio [(Distance ratio %=Time spent in conspecific sector/ total time observed) ×100]. The videos were analysed using Noldus EthoVision® XT17 tracking software (Noldus Information Technologies, Inc., Leesburg, VA, USA).

Novel object recognition task

Behavioural experiments were conducted at between 10 a.m. and 4 p.m. in a 30 × 30 × 30 cm tank with opaque walls and partitions. Before training, each animal was habituated to the experimental apparatus (open field) in the absence of objects for 5 min. In the training phase (phase 1), animals were exposed to two identical cubes (of the same colour) for 10 min. After training, the animals were submitted to a retention interval of 1 h. This separation period is a standard methodological approach used to assess short-term memory, allowing for memory consolidation and preventing immediate recognition effects that could bias the results. In the test (phase 2), a new object (of a different colour) replaced one of the copies of the familiar object and the time spent exploring each object during a period of 10 min was evaluated. The familiar blue objects used in phase 2 were exactly the same ones from phase 1, ensuring continuity in the experimental setup. To avoid a thigmotaxis effect, the distances between the objects and the walls were kept the same. We calculated the exploration time of each object (%). This measurement reflects proximity rather than active exploration based on head orientation. The exploration area was defined as an 8 × 8 cm area centred on the object and preference times were calculated as reported in[29]. The videos were analysed using Noldus EthoVision® XT17 tracking software (Noldus Information Technologies, Inc., Leesburg, VA, USA).

Statistical analysis

Data analysis was performed using GraphPad Prism software (version 9). Statistical tests were selected based on the specific experimental design and are indicated in the corresponding figure legends. Significance thresholds were defined as follows: $*p<0.05$, $**p<0.01$, $***p<0.001$, and $****p<0.0001$. Graphs were generated using GraphPad Prism (version 9).

Data availability

The mass spectrometry proteomics data have been deposited to the ProteomeXchange Consortium via the PRIDE. Nucleic Acids Res 50(D1):D543-D552 (PubMed ID: 34723319).] partner repository with the dataset

identifier PXD058522. Transcriptomics data have been deposited in the ZENODO repository (https://zenodo.org/records/14809944) and (https://zenodo.org/records/15123596).

Received: 4 February 2025; Accepted: 7 July 2025
Published online: 14 July 2025

References

1. Bouhlal, Y., Amouri, R., Euch-Fayeche, E., Hentati, F. & G. & Autosomal recessive spastic ataxia of Charlevoix–Saguenay: An overview. *Parkinsonism Relat. Disord.* **17**, 418–422 (2011).
2. Engert, J. C. et al. ARSACS, a spastic ataxia common in Northeastern québec, is caused by mutations in a new gene encoding an 11.5-kb ORF. *Nat. Genet.* **24**, 120–125 (2000).
3. Anderson, J. F., Siller, E. & Barral, J. M. The neurodegenerative-disease-related protein sacsin is a molecular chaperone. *J. Mol. Biol.* **411**, 870–880 (2011).
4. Anderson, J. F., Siller, E. & Barral, J. M. The Sacsin repeating region (SRR): A novel Hsp90-Related Supra-Domain associated with neurodegeneration. *J. Mol. Biol.* **400**, 665–674 (2010).
5. Ali, Z. et al. Novel SACS mutations associated with intellectual disability, epilepsy and widespread supratentorial abnormalities. *J. Neurol. Sci.* **371**, 105–111 (2016).
6. Schmahmann, J. The cerebellar cognitive affective syndrome. *Brain* **121**, 561–579 (1998).
7. Hoche, F., Guell, X., Vangel, M. G., Sherman, J. C. & Schmahmann, J. D. The cerebellar cognitive affective/schmahmann syndrome scale. *Brain* **141**, 248–270 (2018).
8. Larivière, R. et al. Sacs R272C missense homozygous mice develop an ataxia phenotype. *Mol. Brain.* **12**, 19 (2019).
9. Chen, C., Merrill, R. A., Jong, C. J. & Strack, S. Driving mitochondrial fission improves cognitive, but not motor deficits in a mouse model of Ataxia of Charlevoix-Saguenay. (2024). https://doi.org/10.21203/rs.3.rs-4178088/v1
10. Choi, T. Y., Choi, T. I., Lee, Y. R., Choe, S. K. & Kim, C. H. Zebrafish as an animal model for biomedical research. *Exp. Mol. Med.* **53**, 310–317 (2021).
11. Naef, V. et al. Modeling Sacsin depletion in Danio Rerio offers new insight on retinal defects in ARSACS. *Neurobiol. Dis.* **205**, 106793 (2025).
12. Andreasen, N. C. et al. The cerebellum plays a role in conscious episodic memory retrieval. *Hum. Brain Mapp.* **8**, 226–234 (1999).
13. Pilotto, F., Del Bondio, A. & Puccio, H. Hereditary ataxias: From bench to clinic. Where do we stand? *Cells*. **13**, 319 (2024).
14. Cuevas, E. et al. Tauroursodeoxycholic acid (TUDCA) is neuroprotective in a chronic mouse model of parkinson's disease. *Nutr. Neurosci.* **25**, 1374–1391 (2022).
15. Naef, V. et al. Efficient neuroprotective rescue of Sacsin-Related disease phenotypes in zebrafish. *Int. J. Mol. Sci.* **22**, 8401 (2021).
16. Weng, J. et al. Tauroursodeoxycholic acid inhibited apoptosis and oxidative stress in H_2O_2-Induced BMSC death via modulating the Nrf-2 signaling pathway: The therapeutic implications in a rat model of spinal cord injury. *Mol. Neurobiol.* **61**, 3753–3768 (2024).
17. Chen, C., Merrill, R. A., Jong, C. J. & Strack, S. Driving mitochondrial fission improves cognitive, but not motor deficits in a mouse model of Ataxia of Charlevoix-Saguenay. *Res. Sq.* https://doi.org/10.21203/rs.3.rs-4178088/v1 (2024).
18. Stewart, A. M., Gaikwad, S., Kyzar, E. & Kalueff, A. V. Understanding spatio-temporal strategies of adult zebrafish exploration in the open field test. *Brain Res.* **1451**, 44–52 (2012).
19. dos Santos, C. P., de Oliveira, M. N., Silva, P. F. & Luchiari, A. C. Relationship between boldness and exploratory behavior in adult zebrafish. *Behav. Processes*. **209**, 104885 (2023).
20. Tamaš, O. et al. Social cognition in patients with cerebellar neurodegenerative disorders. *Front Syst. Neurosci* **15**, (2021).
21. Verhoeven, W. M. A. et al. Cerebellar cognitive affective syndrome and autosomal recessive spastic Ataxia of Charlevoix-Saguenay: A report of two male Sibs. *Psychopathology* **45**, 193–199 (2012).
22. Mignarri, A. et al. Cerebellum and neuropsychiatric disorders: Insights from ARSACS. *Neurol. Sci.* **35**, 95–97 (2014).
23. Ogi, A. et al. Social preference tests in zebrafish: A systematic review. *Front Vet. Sci* **7**, (2021).
24. Hosaka, S., Hosokawa, M., Hibi, M. & Shimizu, T. The Zebrafish cerebellar neural circuits are involved in orienting behavior. *eneuro* **11**, ENEURO.0141-24.2024 (2024).
25. Nunes, A. R., Ruhl, N., Winberg, S. & Oliveira, R. F. Social phenotypes in Zebrafish. In *The rights and wrongs of zebrafish: Behavioral phenotyping of zebrafish* 95–130 (Springer, 2017). https://doi.org/10.1007/978-3-319-33774-6_5
26. Hamilton, T. J., Krook, J., Szaszkiewicz, J. & Burggren, W. Shoaling, boldness, anxiety-like behavior and locomotion in zebrafish (Danio rerio) are altered by acute benzo[a]pyrene exposure. *Sci. Total Environ.* **774**, 145702 (2021).
27. Guenther, G. et al. First report of spastic ataxia of Charlevoix-Saguenay cases in mexico. Novel SACS gene mutations identified. *Neurol. Perspect.* **2**, 214–223 (2022).
28. Krygier, M. & Mazurkiewicz-Bełdzińska, M. Milestones in genetics of cerebellar ataxias. *Neurogenetics* **22**, 225–234 (2021).
29. Gaspary, K. V., Reolon, G. K., Gusso, D. & Bonan, C. D. Novel object recognition and object location tasks in zebrafish: Influence of habituation and NMDA receptor antagonism. *Neurobiol. Learn. Mem.* **155**, 249–260 (2018).
30. Pinheiro-da-Silva, J., Silva, P. F., Nogueira, M. B. & Luchiari, A. C. Sleep deprivation effects on object discrimination task in zebrafish (Danio rerio). *Anim. Cogn.* **20**, 159–169 (2017).
31. May, Z. et al. Object recognition memory in zebrafish. *Behav. Brain Res.* **296**, 199–210 (2016).
32. Criscuolo, C. et al. Powerhouse failure and oxidative damage in autosomal recessive spastic ataxia of Charlevoix-Saguenay. *J. Neurol.* **262**, 2755–2763 (2015).
33. Girard, M. et al. Mitochondrial dysfunction and purkinje cell loss in autosomal recessive spastic ataxia of Charlevoix-Saguenay (ARSACS). *Proc. Natl. Acad. Sci.* **109**, 1661–1666 (2012).
34. Morani, F. et al. Integrative Organelle-Based functional proteomics: In Silico prediction of impaired functional annotations in SACS KO cell model. *Biomolecules* **12**, 1024 (2022).
35. Morani, F. et al. Functional transcriptome analysis in ARSACS KO cell model reveals a role of Sacsin in autophagy. *Sci. Rep.* **9**, 11878 (2019).
36. Lananna, B. V. & Musiek, E. S. The wrinkling of time: Aging, inflammation, oxidative stress, and the circadian clock in neurodegeneration. *Neurobiol. Dis.* **139**, 104832 (2020).
37. Galatolo, D. et al. Proteomics and lipidomic analysis reveal dysregulated pathways associated with loss of Sacsin. *Front. Neurosci.* **18**, 1375299 (2024).
38. Ruttkay-Nedecky, B. et al. The role of Metallothionein in oxidative stress. *Int. J. Mol. Sci.* **14**, 6044–6066 (2013).
39. Ling, X. B. et al. Mammalian Metallothionein-2A and oxidative stress. *Int. J. Mol. Sci.* **17**, (2016).
40. Tolomeo, M. et al. Retrograde response to mitochondrial dysfunctions associated to LOF variations in FLAD1 exon 2: Unraveling the importance of RFVT2. *Free Radic. Res.* **56**, 511–525 (2022).
41. García-Villoria, J. et al. FLAD1, encoding FAD synthase, is mutated in a patient with myopathy, scoliosis and cataracts. *Clin. Genet.* **94**, 592–593 (2018).
42. Cleveland, B. M., Leonard, S. S., Klandorf, H. & Blemings, K. P. Urate oxidase knockdown decreases oxidative stress in a murine hepatic cell line. *Oxid. Med. Cell. Longev.* **2**, 93–98 (2009).

43. Uszczynska-Ratajczak, B. et al. Profiling subcellular localization of nuclear-encoded mitochondrial gene products in zebrafish. *Life Sci. Alliance*. **6**, e202201514 (2023).
44. David, F. et al. Mitochondrial ribosomal protein MRPS15 is a component of cytosolic ribosomes and regulates translation in stressed cardiomyocytes. *Int. J. Mol. Sci.* **25**, 3250 (2024).
45. Peng, C. et al. Ablation of vacuole protein sorting 18 (Vps18) gene leads to neurodegeneration and impaired neuronal migration by disrupting multiple vesicle transport pathways to lysosomes. *J. Biol. Chem.* **287**, 32861–32873 (2012).
46. Guo, J., Johansson, I., Mkrtchian, S. & Ingelman-Sundberg, M. The CYP2W1 enzyme: Regulation, properties and activation of prodrugs. *Drug Metab. Rev.* **48**, 369–378 (2016).
47. He, H., Bing, H. & Liu, G. TSR2 induces laryngeal cancer cell apoptosis through inhibiting NF-κB signaling pathway. *Laryngoscope* **128**, (2018).
48. Fatica, T. et al. TRNT-1 deficiency is associated with loss of tRNA integrity and imbalance of distinct proteins. *Genes (Basel)*. **14**, 1043 (2023).
49. Giannelou, A. et al. Aberrant tRNA processing causes an autoinflammatory syndrome responsive to TNF inhibitors. *Ann. Rheum. Dis.* **77**, 612–619 (2018).
50. Serna, M. et al. The structure of the TBCE/TBCB chaperones and α-tubulin complex shows a tubulin dimer dissociation mechanism. *J. Cell. Sci.* https://doi.org/10.1242/jcs.167387 (2015).
51. Sun, Y., Koyama, Y. & Shimada, S. Inflammation from peripheral organs to the brain: How does systemic inflammation cause neuroinflammation? *Front Aging Neurosci.* **14**, (2022).
52. Kawahata, I. & Fukunaga, K. Pathogenic impact of fatty Acid-Binding proteins in parkinson's Disease—Potential biomarkers and therapeutic targets. *Int. J. Mol. Sci.* **24**, 17037 (2023).
53. Kagawa, Y. et al. Fatty Acid-Binding protein 4 is essential for the inflammatory and metabolic response of microglia to lipopolysaccharide. *J. Neuroimmune Pharmacol.* **18**, 448–461 (2023).
54. Ugalde, C. et al. Mutated ND2 impairs mitochondrial complex I assembly and leads to Leigh syndrome. *Mol. Genet. Metab.* **90**, 10–14 (2007).
55. Courtois, S. et al. Mutation on MT-CO2 gene induces mitochondrial disease associated with neurodegeneration and intracerebral iron accumulation (NBIA). *Biochim. Biophys. Acta Mol. Basis Dis.* **1870**, 166856 (2024).
56. Shyrokova, E. Y., Prassolov, V. S. & Spirin, P. V. The role of the MCTS1 and DENR proteins in regulating the mechanisms associated with malignant cell transformation. *Acta Naturae*. **13**, 98–105 (2021).
57. Gao, Y. et al. β2-microglobulin functions as an endogenous NMDAR antagonist to impair synaptic function. *Cell* **186**, 1026–1038e20 (2023).
58. Wang, H., Liu, B. & Wei, J. Beta2-microglobulin(B2M) in cancer immunotherapies: Biological function, resistance and remedy. *Cancer Lett.* **517**, 96–104 (2021).
59. Ryan, T. A., Tumbarello, D. A. & Optineurin A coordinator of Membrane-Associated cargo trafficking and autophagy. *Front Immunol.* **9**, (2018).
60. Li, R. et al. Heme-hemopexin complex attenuates neuronal cell death and stroke damage. *J. Cereb. Blood Flow. Metab.* **29**, 953–964 (2009).
61. Won, J. Y. et al. Novel loss-of-function variants of TRAPPC2 manifesting X-linked spondyloepiphyseal dysplasia tarda: Report of two cases. *BMC Med. Genet.* **20**, 70 (2019).
62. Scrivens, P. J. et al. TRAPPC2L is a novel, highly conserved TRAPP-Interacting protein. *Traffic* **10**, 724–736 (2009).
63. Ansar, M. et al. Bi-allelic variants in DYNC1I2 cause syndromic microcephaly with intellectual disability, cerebral malformations, and dysmorphic facial features. *Am. J. Hum. Genet.* **104**, 1073–1087 (2019).
64. Yoon, Y. M. et al. Tauroursodeoxycholic acid reduces ER stress by regulating of Akt-dependent cellular prion protein. *Sci. Rep.* **6**, 39838 (2016).
65. Koebis, M. et al. LAMP5 in presynaptic inhibitory terminals in the hindbrain and spinal cord: A role in startle response and auditory processing. *Mol. Brain*. **12**, 20 (2019).
66. Spencer, Z. T. et al. The USP46 deubiquitylase complex increases wingless/wnt signaling strength by stabilizing Arrow/LRP6. *Nat. Commun.* **14**, 6174 (2023).
67. Roche, J. P., Packard, M. C., Moeckel-Cole, S. & Budnik, V. Regulation of synaptic plasticity and synaptic vesicle dynamics by the PDZ protein scribble. *J. Neurosci.* **22**, 6471–6479 (2002).
68. Ezan, J. et al. Neuron-Specific deletion of scrib in mice leads to neuroanatomical and locomotor deficits. *Front Genet* **13**, (2022).
69. Dauar, M. T. et al. Characterization of the contactin 5 protein and its risk-associated polymorphic variant throughout the alzheimer's disease spectrum. *Alzheimer's Dement.* **19**, 2816–2830 (2023).
70. Deneault, E. et al. CNTN5-/+or EHMT2-/+human iPSC-derived neurons from individuals with autism develop hyperactive neuronal networks. *Elife* **8**, (2019).
71. Gazzerro, E. et al. Hyccin, the molecule mutated in the leukodystrophy hypomyelination and congenital cataract (HCC), is a neuronal protein. *PLoS One*. **7**, e32180 (2012).
72. Wang, Y. et al. Genome-wide CRISPR screen reveals CLPTM1L as a lipid scramblase required for efficient glycosylphosphatidylinositol biosynthesis. *Proc. Natl. Acad. Sci.* **119**, (2022).
73. McWilliams, T. G. Fine-tune TMEM11 to unleash basal mitophagy. *J Cell. Biol.* **222**, (2023).
74. Idelfonso-García, O. G. et al. Is Nucleoredoxin a master regulator of cellular redox homeostasis? Its implication in different pathologies. *Antioxidants (Basel Switzerland)* **11**, (2022).
75. Gracie, S. et al. De Novo loss-of-function variant in < scp > *PTDSS1* is associated with developmental delay. *Am. J. Med. Genet. Part. A*. **188**, 1739–1745 (2022).
76. Freitas, I. N. et al. Insights by which TUDCA is a potential therapy against adiposity. *Front Endocrinol. (Lausanne)* **14**, (2023).
77. Wang, S. et al. TUDCA inhibits EV71 replication by regulating ER stress signaling pathway and suppressing autophagy. *Diagn. Microbiol. Infect. Dis.* **110**, 116500 (2024).
78. Tran, B. N. et al. Reduced exploratory behavior in neuronal Nucleoredoxin knockout mice. *Redox Biol.* **45**, 102054 (2021).
79. Zhu, Q. et al. Anterior gradient 2 is induced in cutaneous wound and promotes wound healing through its adhesion domain. *FEBS J.* **284**, 2856–2869 (2017).
80. Zhang, Q. et al. Adipocyte-Derived Exosomal MTTP suppresses ferroptosis and promotes chemoresistance in colorectal Cancer. *Adv. Sci.* **9**, (2022).
81. Handschuh, K. et al. ESCRT-II/Vps25 constrains digit number by Endosome-Mediated selective modulation of FGF-SHH signaling. *Cell. Rep.* **9**, 674–687 (2014).
82. Bartee, E., Mansouri, M., Hovey Nerenberg, B. T., Gouveia, K. & Früh, K. Downregulation of major histocompatibility complex class I by human ubiquitin ligases related to viral immune evasion proteins. *J. Virol.* **78**, 1109–1120 (2004).
83. Nakamura, N., Fukuda, H., Kato, A. & Hirose, S. MARCH-II is a Syntaxin-6–binding protein involved in endosomal trafficking. *Mol. Biol. Cell.* **16**, 1696–1710 (2005).
84. Fregoso, F. E. et al. Molecular mechanism of Arp2/3 complex Inhibition by arpin. *Nat. Commun.* **13**, 628 (2022).
85. Jiang, W. et al. IFI30 as a prognostic biomarker and correlation with immune infiltrates in glioma. *Ann. Transl. Med.* **9**, 1686–1686 (2021).
86. Tremblay, M., Girard-Côté, L., Brais, B. & Gagnon, C. Documenting manifestations and impacts of autosomal recessive spastic ataxia of Charlevoix–Saguenay to develop patient-reported outcome. *Orphanet J. Rare Dis.* **17**, 369 (2022).

87. Rudolph, S. et al. Cognitive-affective functions of the cerebellum. *J. Neurosci.* **43**, 7554–7564 (2023).
88. Zesiewicz, T. A. et al. Comprehensive systematic review summary: Treatment of cerebellar motor dysfunction and ataxia. *Neurology* **90**, 464–471 (2018).
89. Ayyar, V. S. & Sukumaran, S. Circadian rhythms: Influence on physiology, pharmacology, and therapeutic interventions. *J. Pharmacokinet. Pharmacodyn.* **48**, 321–338 (2021).
90. Xu, X., Wang, J. & Chen, G. Circadian cycle and neuroinflammation. *Open Life Sci.* **18**, (2023).
91. Leng, Y., Musiek, E. S., Hu, K., Cappuccio, F. P. & Yaffe, K. Association between circadian rhythms and neurodegenerative diseases. *Lancet Neurol.* **18**, 307–318 (2019).
92. Zielinski, M. R., Gibbons, A. J. & Neuroinflammation sleep, and circadian rhythms. *Front Cell. Infect. Microbiol.* **12**, (2022).
93. Kim, J. & Sun, W. Circadian coordination: Understanding interplay between circadian clock and mitochondria. *Anim. Cells Syst. (Seoul)*. **28**, 228–236 (2024).
94. Lunnon, K. et al. Mitochondrial genes are altered in blood early in alzheimer's disease. *Neurobiol. Aging.* **53**, 36–47 (2017).
95. Ball, M., Thorburn, D. R. & Rahman, S. *Mitochondrial DNA-Associated Leigh Syndrome Spectrum*. *GeneReviews®* 20301352. (1993).
96. Dagar, S. et al. Ribosome profiling and mass spectrometry reveal widespread mitochondrial translation defects in a striatal cell model of huntington disease. *Mol. Cell. Proteom.* **23**, 100746 (2024).
97. Mezhnina, V., Ebeigbe, O. P., Poe, A. & Kondratov, R. V. Circadian control of mitochondria in reactive oxygen species homeostasis. *Antioxid. Redox Signal.* **37**, 647–663 (2022).
98. Rosa, A. I. et al. Novel insights into the antioxidant role of Tauroursodeoxycholic acid in experimental models of parkinson's disease. *Biochim. Biophys. Acta Mol. Basis Dis.* **1863**, 2171–2181 (2017).
99. Keene, C. D. et al. Tauroursodeoxycholic acid, a bile acid, is neuroprotective in a transgenic animal model of Huntington's disease. *Proc. Natl. Acad. Sci.* **99**, 10671–10676 (2002).
100. Wu, M. et al. Molecular mechanism and therapeutic strategy of bile acids in alzheimer's disease from the emerging perspective of the microbiota–gut–brain axis. *Biomed. Pharmacother.* **178**, 117228 (2024).
101. Lu, X. et al. Tauroursodeoxycholic acid produces antidepressant-like effects in a chronic unpredictable stress model of depression via Attenuation of neuroinflammation, oxido-nitrosative stress, and Endoplasmic reticulum stress. *Fundam Clin. Pharmacol.* **32**, 363–377 (2018).
102. Kim, S. J. et al. Anti-inflammatory effect of Tauroursodeoxycholic acid in RAW 264.7 macrophages, bone marrow-derived macrophages, BV2 microglial cells, and spinal cord injury. *Sci. Rep.* **8**, 3176 (2018).
103. Makowski, L. & Hotamisligil, G. S. Fatty acid binding proteins—the evolutionary crossroads of inflammatory and metabolic responses. *J. Nutr.* **134**, 2464S–2468S (2004).
104. Tomida, S. et al. Usp46 is a quantitative trait gene regulating mouse immobile behavior in the tail suspension and forced swimming tests. *Nat. Genet.* **41**, 688–695 (2009).
105. Imai, S. et al. Ubiquitin-Specific peptidase 46 (Usp46) regulates mouse immobile behavior in the tail suspension test through the GABAergic system. *PLoS One.* **7**, e39084 (2012).
106. Royes, J. A. B. & Chapman, F. A. Preparing your own fish feeds. *EDIS* (1969). (2003).
107. Licitra, R. et al. Zebrafish feed intake: A systematic review for standardizing feeding management in laboratory conditions. *Biology (Basel)*. **13**, 209 (2024).
108. Cachat, J. M. et al. Video-Aided Analysis of Zebrafish Locomotion and Anxiety-Related Behavioral Responses. in 1–14 (2011). https://doi.org/10.1007/978-1-60761-953-6_1
109. Cachat, J. et al. Measuring behavioral and endocrine responses to novelty stress in adult zebrafish. *Nat. Protoc.* **5**, 1786–1799 (2010).
110. Liu, C. et al. CRISPR/Cas9-induced shank3b mutant zebrafish display autism-like behaviors. *Mol. Autism.* **9**, 23 (2018).

Acknowledgements

The authors thank the Fondation de l'Ataxie Charlevoix-Saguenay and the the Italian patients' association (ARSACS OdV) for their constant encouragement and support. We acknowledge the editorial support of Dr. Catherine J. Wrenn for expert language editing.

Author contributions

V.N. -Writing – original draft, Visualization, Validation, Supervision, Project administration, Methodology, Investigation, Funding Acquisition, Formal analysis, Data curation, Conceptualization. S.DV.- review & editing. M.G.- Visualization & Data curation. R.L.- Methodology. T. B.-Visualization, Formal analysis & Data curation. G. CV. - Methodology. M.P.- Methodology. F.M.S. -Writing – review & editing, Supervision & Funding acquisition.

Funding

This work was supported by Fondation de l'Ataxie Charlevoix-Saguenay (seed grant 2022 to V.N.) and in part by Ministero della Salute, Grant RC2024-25 and 5×1000 (F.M.S., S.D.V., V.N. and M.G) and grant RF-2019-12370417 UO3 (F.M.S.).

Declarations

Competing interests

The authors declare no competing interests.

Ethics approval

This study does not include human samples. All animal procedures were authorized by the University of Pisa Animal Ethics Committee and the Italian Ministry of Health (n° 620/2024-PR). The study is reported in accordance with ARRIVE guidelines.

Additional information

Supplementary Information The online version contains supplementary material available at https://doi.org/10.1038/s41598-025-10850-0.

Correspondence and requests for materials should be addressed to V.N. or F.M.S.